University of Wollongong
Research Online

Australian Institute for Innovative Materials - Papers

Australian Institute for Innovative Materials

2006

Comparison of small-field behaviour in MgB2, low and high temperature superconductors

Alexey V. Pan
University of Wollongong, pan@uow.edu.au

S X. Dou
University of Wollongong, shi@uow.edu.au

Publication Details

Pan, AV & Dou, SX (2006), Comparison of small-field behaviour in MgB2, low and high temperature superconductors, Physical Review B (Condensed Matter and Materials Physics), 73(5), pp. 052506-1-052506-4.

Research Online is the open access institutional repository for the University of Wollongong. For further information contact the UOW Library: research-pubs@uow.edu.au

Comparison of small-field behaviour in MgB2, low and high temperature superconductors

Abstract

Different types of superconductors have been investigated at small magnetic fields (B_a) over wide temperature (T) ranges at different B_a orientations. It has been shown that the temperature dependence of the characteristic field (B^*), separating the B_a-independent critical current density (J_c) plateau (single vortex pinning regime) and the region with $J_c(B_a)$ (collective pinning), can be attributed either to the temperature dependence of the magnetic penetration depth for Nb-film and MgB_2bulk superconductors, or to thermally activated processes for Bi-based superconductors and $YBa_2Cu_3O_{7-\delta}$ superconducting films. In both cases the vortex pinning influence appears to have a secondary role, affecting the effective vortex depinning radius. An exception in such $B^*(T)$ behavior is considered for Nb film when the magnetic field has its considerable component applied perpendicular to the main surface of the film.

Keywords

Comparison, small, field, behaviour, MgB2, low, high, temperature, superconductors

Disciplines

Engineering | Physical Sciences and Mathematics

Publication Details

Pan, AV & Dou, SX (2006), Comparison of small-field behaviour in MgB2, low and high temperature superconductors, Physical Review B (Condensed Matter and Materials Physics), 73(5), pp. 052506-1-052506-4.

This journal article is available at Research Online: http://ro.uow.edu.au/aiimpapers/25

Comparison of small-field behavior in MgB_2, Low- and high-temperature superconductors

Alexey V. Pan and Shi X. Dou
Institute for Superconducting and Electronic Materials, University of Wollongong, Northfields Avenue, Wollongong, NSW 2522, Australia
(Received 27 July 2005; revised manuscript received 28 October 2005; published 27 February 2006)

Different types of superconductors have been investigated at small magnetic fields (B_a) over wide temperature (T) ranges at different B_a orientations. It has been shown that the temperature dependence of the characteristic field (B^*), separating the B_a-independent critical current density (J_c) plateau (single vortex pinning regime) and the region with $J_c(B_a)$ (collective pinning), can be attributed either to the temperature dependence of the magnetic penetration depth for Nb-film and MgB_2 bulk superconductors, or to thermally activated processes for Bi-based superconductors and $YBa_2Cu_3O_{7-\delta}$ superconducting films. In both cases the vortex pinning influence appears to have a secondary role, affecting the effective vortex depinning radius. An exception in such $B^*(T)$ behavior is considered for Nb film when the magnetic field has its considerable component applied perpendicular to the main surface of the film.

DOI: 10.1103/PhysRevB.73.052506 PACS number(s): 74.25.Ha

This work aims to establish factors influencing the crossover field (B^*), separating the applied magnetic field (B_a) independent critical current density (J_c) region from the region with degrading $J_c(B_a)$ behavior, for different types of superconductors, including different high-temperature superconductors (HTS), low-temperature superconductors (LTS), and relatively new magnesium diboride superconductors (MgB_2). In contrast to HTS $YBa_2Cu_3O_{7-\delta}$ (YBCO) films, studies of magnetic behavior in low magnetic fields ($B_a < B^*$) have been rather limited in Bi-based superconductors and no studies have been carried out in MgB_2 superconductors. Generally, the B^* dependence on temperature (T) has been poorly investigated for all types of superconductors.

The electromagnetic behavior of YBCO films in the low-field region has been intensively discussed in terms of factors governing the size of the field independent interval of J_c at $B_a < B^*$.[1–5] The value of B^* has been suggested to be governed by the most effective linear defects. Pinning of vortices on these defects leads to a matching effect, which occurs when the number of vortices corresponds to the number of linear defects in films.[1,2] This matching effect has been shown to be strongly influenced by thermally activated processes, which have been suggested to explain the dependence of B^* on temperature (T).[5]

The low-field behavior of J_c in Bi-based superconductors is usually associated with a sharp drop at low fields[6] due to the breaking of weak links between superconducting grains, where the superconducting order parameter is suppressed, creating channels for vortex motion. Recent works on YBCO films,[5] Bi tapes,[7] and Bi-single crystals[8] have suggested that thermally activated depinning could play a similar role in the $B^*(T)$ behavior in these materials. YBCO and Bi-based materials have distinctly different microstructures and nanostructures, and these differences are even more pronounced for their most practically promising forms, such as YBCO films and Bi tapes. Therefore, establishing common features in their electromagnetic behavior would advance understanding not only of their pinning mechanisms, but also of their technological needs.

Conventional LTS, as well as HTS, are unambiguously described to obey the single vortex pinning (SVP) regime within the J_c independent region at low fields and a collective pinning regime with $J_c(B_a)$ at higher fields at which intervortex interactions become important.[9] In light of this fact, it was assumed that the temperature dependence of the crossover field B^* between these pinning regimes would depend on temperature dependence of vortex-vortex interactions, i.e., on the magnetic penetration depth λ.[5] However, no experimental confirmation was provided for this assumption. Moreover, it is unclear whether the $B^*(T)$ behavior in HTS and LTS would have similar features.

As to the MgB_2 superconductor, no detailed study of the low-field region in the MgB_2 superconductor is yet available. On the one hand, one can anticipate similar behavior for $B^*(T)$ and $J_c(B_a)$ in small fields to that of LTS. Indeed, MgB_2 has been shown to be more akin to metallic LTS than to copper oxide HTS.[10] On the other hand, the presence of weak links in MgB_2, which can significantly degrade current carrying abilities in MgB_2 [similarly to HTS (Refs. 6 and 11)], cannot be completely ruled out even at low fields. Two drops in the J_c behavior as a function of B_a that are associated with weak links have been revealed in MgB_2.[12–15] The second drop at fields close to the irreversibility field has already been addressed.[12,15] The first low-field drop was treated in terms of superconducting screening on the scale of large grains.[12,15] However, its influence on the SVP regime and B^* behavior is unclear. In fact, the SVP regime and $B^*(T)$ have not yet been described for MgB_2 at all.

In this work, we deal with issues raised above, analyzing the low-field region of $J_c(B_a)$ dependences in LTS Nb film, HTS YBCO films and Bi-based materials, and MgB_2 samples. We also discuss general mechanisms leading to the $B^*(T)$ behavior observed.

In Table I we list the samples investigated and some of their characteristics. More details on properties and dimensions of the measured Nb-film (NbF) can be found elsewhere.[16] Two typical MgB_2 bulk samples have slightly different J_c due to different preparation conditions.[15] The MB1 dimensions are $2.7 \times 1.45 \times 0.47$ mm^3; MB2 is cubic $\simeq 0.5^3$ mm^3. The measured YBCO films were grown by

 ©2006 The American Physical Society

TABLE I. Investigated samples and their available superconducting parameters.

Sample	d_p, μm	T_c, K	J_c, 10^{10} A/m^2	$\lambda(0)$, nm	$r_{dp}(0)$, nm	x	q
NbF	0.12	8.9	1.5[a]	100[16]	155	—	—
MB1	470	38.9	0.72[b]	140[17]	137	—	—
MB2	440	37.56	0.5[b]	140[17]	168	—	—
K1509	0.3	86.7	2.9[c]	180[18]	205	1.5	2.5
K21	0.3	86.3	2.4[c]	180[18]	220	1.5	2.5
PP17	0.3	87.9	2.7[c]	180[18]	320	1.5	2.5
PP18	0.18	85.7	1.3[c]	180[18]	290	1.5	2.5
P0311	0.4	89.6	5.2[c]	180[18]	240	1.5	2.5
M	0.3	87.4	0.67[c]	180[18]	86	1.5	2.5
BiC	70	110	0.05[b]	200[19]	200	4.4	5.3
BiMF	380	110	0.03[d]	200[19]	220	7.0	8.0

[a] J_c at T=5 K.
[b] J_c at T=20 K.
[c] J_c at T=70 K.
[d] J_c at T=77 K. d_p denotes sample thickness of the smallest dimension of a sample.

magnetron sputtering (K1509, K21) and by pulsed laser deposition (PP17, PP18, P0311, M).[20,21] All the films were rectangular with the area (length$\times$width) equal to 3 to 9 mm^2. $Bi_2Sr_2Ca_2Cu_3O_{10+\delta}$ samples include typical multifilamentary (BiMF) Ag-sheathed tape ($\sim$4 mm long)[6] and the extracted core of a monocore Ag-sheathed tape (BiC),[7] being $\sim 3\times 3\times 0.3$ mm^3.

The majority of $J_c(B_a)$ curves has been obtained from magnetization loops measured with the help of a SQUID magnetometer. In the case of the Nb film, a capacitive torque magnetometer has been used.[16] The samples were measured at different orientations (θ) between main sample surfaces and B_a, so that θ=0° defines B_a parallel to the surface. Angles were defined with an accuracy of $<\pm 5°$ for all the samples. The magnetic measurements rule out the self-field influence observed upon transport current measurements in fields smaller than the first penetration field for samples with relatively small demagnetizing factor, such as BiMF.[22]

Typical $J_c(B_a,T)$ dependences are shown in Fig. 1 for a MgB_2 bulk sample and an YBCO film. Typical $J_c(B)$ dependences for Bi and Nb samples can respectively be found in Refs. 7 and 16, for YBCO films at different orientations in Ref. 5.

In Fig. 2 we show characteristic field B^* dependences as a function of reduced temperature ($t=T/T_c$ with T_c being the critical temperature) for some of the measured samples. B^* is defined as the 0.5% deviation of J_c from the corresponding $J_{c0}\simeq J_c(B_a=0)$ value (Fig. 1).

Strikingly, all the $B^*(t)$ dependences for different samples are arranged in two clearly defined groups with (i) negative curvature for HTS samples and (ii) linear behavior for MgB_2 and Nb samples. Generally, the negative curvature for HTS samples is independent of the B_a orientation. The linear behavior is also independent of orientation for MgB_2 samples, whereas Nb film exhibits a negative curvature if the field is applied at a considerable angle to the main film surface(θ =30° in Fig. 2).

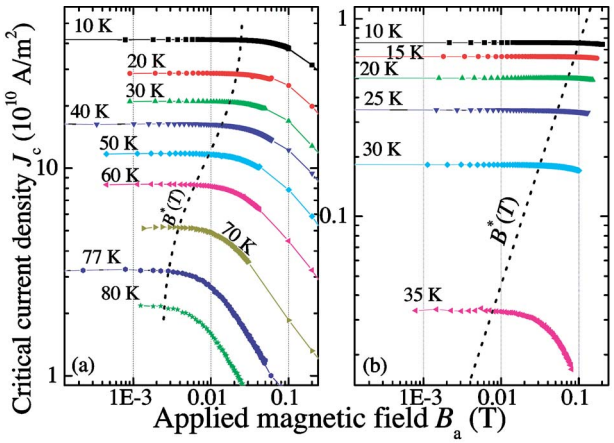

FIG. 1. (Color online) $J_c(B_a)$ dependences for (a) YBCO (P0311) and (b) MgB_2 (MB2) samples. The dotted lines show $B^*(T)$.

The key message delivered by the observation as discussed below is as follows. The linear behavior is well consistent with the temperature dependence of the magnetic field penetration depth $\lambda(T)$, whereas the negative curvature is in line with thermally activated processes known for HTS. A special case should be considered for the behavior of the Nb film in fields applied at θ considerably $>0°$.

In the SVP regime the intervortex spacing (a_0) significantly exceeds the radius of the vortex-vortex interaction [$\simeq 2\lambda(T)$]. Hence, vortices can be pinned at a first available metastable pinning center. The intervortex spacing is given by $a_0\simeq(\Phi_0/B_a)^{1/2}$, where Φ_0 is the flux quantum. As the field increases, vortices start to interact with each other at $a_0\simeq 2\lambda(T)$. Eventually, vortices rearrange themselves from their metastable positions to a flux-line lattice (FLL) configuration, when a_0 is reduced to the radius of the depinning onset r_{dp}. In this case, r_{dp} is a measure of depinning for individual vortices in a superconductor at low fields. In the

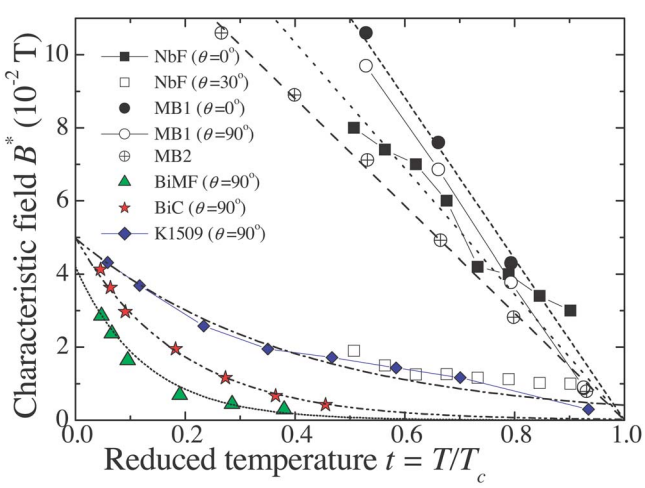

FIG. 2. (Color online) Characteristic field $B^*(T)$ dependences. The dotted and dashed lines are fits of Eq. (3) to the corresponding data.

simplest case, the $B^*(T)$ dependence should solely be governed by the $\lambda(T)$ behavior, since $a_0 = r_{dp} \propto \lambda(T)$. In an extreme case of weak pinning $r_{dp} \simeq 2\lambda(T)$. Within the frame of the Ginzburg-Landau theory $\lambda(T) \simeq \lambda(0)[2(1-t)]^{-1/2}$, where $\lambda(0)$ is the penetration depth at $T=0$ K. Thus, at the crossover from the SVP regime to the FLL regime ($B_a \simeq B^*$), one obtains[5]

$$B^*(t) \simeq \frac{\Phi_0}{r_{dp}^2(0)}[2(1-t)]. \quad (1)$$

Experimentally, we find that Eq. (1) can readily fit the group of linear curves for Nb and MgB_2 samples in Fig. 2 with $r_{dp}(0)$ as the only fitting parameter. Radii of the individual depinning $r_{dp}(0)$ obtained from the fitting procedure for the Nb film in the field applied at $\theta=0°$ and for the MgB_2 samples are given in Table I.

A larger r_{dp} and smaller values of $B^*(t)$ have been obtained for MB2 than for sample MB1. Taking into account a smaller J_c for MB2 (Table I), these results can be attributed to a weaker pinning contribution to the FLL arrangement for MB2. For the cubic MB2 sample, $B^*(t)$ curves measured with B_a along any of the three sample dimensions coincide. For the rectangular sample MB1, $B^*(t)$ is slightly larger for the field applied along the longest sample dimension (l_p) than that for the field applied along the shortest one (d_p). This is presumably due to a larger influence of the surface pinning if B_a is applied at $\theta=0°$; and/or due to a larger demagnetizing effect if B_a is applied at $\theta=90°$, forcing vortices to interact at slightly lower fields.

For the Nb film measured at $\theta=0°$, the $B^*(t)$ dependence is also well fitted with Eq. (1). The ratio $r_{dp}(0)/\lambda(0)=1.55$, $\lambda(0) \sim 100$ nm.[16] This ratio is larger than that for the MgB_2 samples (Table I).

Thus, for the "linear" group in Fig. 2, $B^*(T) \propto \lambda(T)$ with pinning playing the secondary role, adjusting r_{dp}. No influence of weak links or thermally activated processes should be invoked.

A special case should be considered for the $B^*(t)$ curve measured at $\theta=30°$ for the Nb film (Fig. 2). Indeed, it shows negative curvature in contrast to the dependence at $\theta=0°$. $B^*(t)$ could not be measured for $\theta \to 90°$ for the Nb film because of strong thermomagnetic instabilities (flux jumps) at $\theta > 30°$.[23] The qualitative change in $B^*(t)$ behavior might be attributed to a large demagnetizing factor experienced by the perpendicular component of B_a, and, possibly, to microscopic flux-jumps indistinguishable upon "global" magnetization measurements at $\theta=30°$.

In the case of all the HTS measured in this work, all the $B^*(t)$ curves have negative curvature. The linear fit is inappropriate, implying a different mechanism responsible for the crossover between the SVP and FLL regimes to that described above for the Nb and MgB_2 samples. A similar behavior for HTS samples have been observed in Refs. 5, 7, and 24, it turned out that $B^*(t)$ curves for HTS can be fitted by one of the following functions

$$B^*(t) = B^*(0)(1-t)^x, \quad (2)$$

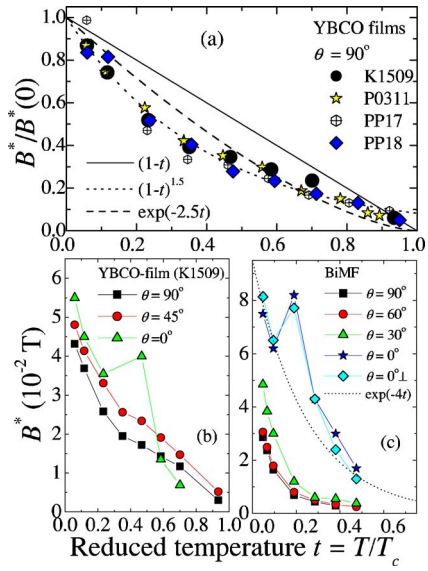

FIG. 3. (Color online) (a) Normalized $B^*(t)$ dependences for YBCO films measured. $B^*(t)$ for (b) YBCO film (K1509) and (c) BiMF sample obtained at different θ.

$$B^*(t) = B^*(0)\exp(-qt), \quad (3)$$

where x and q are pinning-related parameters. These functions have been shown to describe thermally activated depinning processes in different HTSs.[25–28] Indeed, in a general case the $B^*(T)$ dependence would be driven not only by the interplay between (i) vortex-vortex interaction and (ii) pinning, but also by (iii) vortex line tension and (iv) thermal excitation. Moreover, it was shown that the crossover field from SVP regime to the small vortex bundle regime for HTS is $B^*(T) \propto J_c(T)$,[19] where $J_c(T)$ can be $\propto \exp(-t)$ for HTS in general[19] or $\propto (1-t)^x$ for YBCO films in particular.[25] Apparently, the use of each function should depend on a prevailing pinning mechanism in the considered HTS sample. Therefore, any of Eqs. (2) and (3) can be adopted to describe $B^*(t)$ in terms of thermally activated depinning. In any case, the vortex rearrangement at $B^*(T)$ can be considered as the crossover from the SVP regime to the FLL regime (or the small bundle regime) with $J_c(B_a)$ dependence.

Table I provides x and q values obtained after fitting procedures for HTS samples. It turns out that both YBCO films and Bi samples can be better fitted by Eq. (3) than by Eq. (2). In Fig. 2, only exponential fits are shown. In Fig. 3(a), we show a comparison between fits obtained by Eqs. (1)–(3). Generally, YBCO samples have smaller values of the x and q parameters than Bi samples. A slower $B^*(t)$ decrease for YBCO samples can be explained by more efficient pinning of individual vortices in this material. Bi materials are known to be highly susceptible to thermal activations due to their high anisotropy.

In the absence of thermal activations, the relation $r_{dp}(0) = a_0 \simeq [\Phi_0/B^*(0)]^{1/2}$ is still valid. Therefore, we can find $r_{dp}(0)$, which is the second fitting parameter, after substituting $B^*(0)$ into Eqs. (2) and (3). Table I provides the so-obtained values of $r_{dp}(0)$ and corresponding λ taken from the

literature. Surprisingly, for YBCO films and Bi-based samples the smallest $r_{dp}(0)$ (strongest pinning for individual vortices) is obtained for samples with the lowest J_{c0} (M and BiC, respectively); and in the case of YBCO films no apparent B^* dependence on J_{c0} has been established. This indicates that (i) the "effective" pinning for individual vortices at $B_a \leqslant B^*$ is not necessarily the same as in the collective (FLL) pinning region ($B_a > B^*$); (ii) J_c at $B_a \leqslant B^*$ is mainly restricted by the transparency of supercurrent paths (via grain boundaries), not by the pinning.[4,29]

The study of the $B^*(t)$ dependence on θ has shown that the behavior does not undergo a qualitative change for the HTS samples measured [Fig. 3(b) and 3(c)]. With increasing θ, B^* becomes larger for all HTS samples, with the most pronounced enhancement observed for the BiMF sample. The larger B^* can indicate the influence of numerous factors, such as less pronounced anisotropy effects, pinning enhancement through surface pinning and intrinsic pinning, reduced demagnetizing effect, etc. A weaker sensitivity of $B^*(t)$ to the field orientation in the YBCO film can indicate weaker influence of these factors on its behavior. The discontinuities in the $B^*(t)$ behavior at $t \simeq 0.2$ for the BiMF tape and at $t \simeq 0.47$ for the YBCO film at $\theta \simeq 0°$ are not yet completely understood and will be discussed elsewhere. We just note that the discontinuity might be related to the screening effect of the B_a component parallel to the sample surface or, more likely, to another abrupt change in pinning properties at this temperature.

The influence of the demagnatization effect on the orientation dependence is expected to be less pronounced for HTS samples compared to Nb film. This is because thermal activation processes dominate for HTS at $T > 0$ K, reducing demagnetizetion as a consequence of an easier flux penetration and masking possible flux jumps.[23]

In summary, $B^*(T)$ curves for all types of the measured samples are the crossover lines from the SVP regime to the FLL pinning regime. In the case of the Nb film and MgB_2 superconductors with the linear $B^*(T)$ dependence, the crossover and accompanying FLL arrangement is mainly driven by the intervortex interactions, i.e., by $\lambda(T)$, whereas for the HTS, the negative $B^*(T)$ curvature is governed by thermally activated processes. This would mean that the matching effect scenario suggested in Ref. 1 can be applicable only at $T \to 0$ K, when thermal activations are negligible.[5] Generally, at $B_a \leqslant B^*$, r_{dp} for different films may not depend on their J_{c0}. This indicates that the "effective" pinning for individual vortices at $B_a \leqslant B^*$ is not necessarily the same as in the collective pinning region ($B_a > B^*$). J_c at $B_a \leqslant B^*$ is mainly restricted by the transparency of supercurrent paths, not by the pinning. Overall, $r_{dp}(0) \simeq \lambda(0)$ for all samples.

We thank T. Silver for critical remarks. This work is financially supported by the Australian Research Council.

[1] B. Dam *et al.*, Nature (London) **399**, 439 (1999).
[2] F. C. Klaassen *et al.*, Phys. Rev. B **64**, 184523 (2001).
[3] V. M. Pan and A. V. Pan, Fiz. Nizk. Temp. **27**, 991 (2001) [Low Temp. Phys. **27**, 732 (2001)].
[4] V. M. Pan *et al.*, IEEE Trans. Appl. Supercond. **13**, 3714 (2003).
[5] A. V. Pan *et al.*, Physica C **407**, 10 (2004).
[6] J. Horvat *et al.*, Physica C **271**, 51 (1996).
[7] A. V. Pan, S. X. Dou, and H. K. Liu, Physica C **388-389**, 405 (2003).
[8] X. L. Wang *et al.*, J. Appl. Phys. **97**, 10B114 (2005).
[9] A. I. Larkin and Yu. N. Ovchinnikov, Zh. Eksp. Teor. Fiz. **61**, 1221 (1971); **65**, 1704 (1973) [Sov. Phys. JETP **38**, 854 (1974)].
[10] D. Larbalestier *et al.*, Nature (London) **410**, 186 (2001).
[11] H. Hilgenkamp and J. Mannhart, Rev. Mod. Phys. **74**, 485 (2002).
[12] J. Horvat *et al.*, J. Appl. Phys. **96**, 4342 (2004).
[13] S. X. Dou *et al.*, J. Appl. Phys. **94**, 1850 (2003).
[14] M. Eisterer, M. Zehetmayer, and H. W. Weber, Phys. Rev. Lett. **90**, 247002 (2003).
[15] A. V. Pan *et al.*, Supercond. Sci. Technol. **16**, 639 (2003).
[16] A. V. Pan *et al.*, Physica C **301**, 72 (1998).
[17] J. R. Thompson *et al.*, Supercond. Sci. Technol. **14**, L17 (2001).
[18] S. Djordjevic *et al.*, Eur. Phys. J. B **25**, 407 (2002).
[19] G. Blatter *et al.*, Rev. Mod. Phys. **66**, 1125 (1994).
[20] D. A. Luzhbin *et al.*, Phys. Rev. B **69**, 024506 (2004).
[21] A. V. Pan (unpublished).
[22] N. Nakamura, G. D. Gu, and N. Koshizuka, Physica C **225**, 65 (1994); J. Lehtonen *et al.*, *ibid.* **403**, 257 (2004).
[23] P. Esquinazi *et al.*, in *Physics and Materials Science of Vortex States, Flux Pinning and Dynamics*, Vol. 356 of NATO Science Series E, edited by R. Kossowsky *et al.* (Kluwer, Dordrecht, 1999), p. 149.
[24] Yu. V. Fedotov *et al.*, Fiz. Nizk. Temp. **28**, 245 (2001) [Low Temp. Phys. **28**, 172 (2001)].
[25] M. Ziese and P. Esquinazi, Z. Phys. B: Condens. Matter **94**, 265 (1994).
[26] L. Miu, Phys. Rev. B **46**, 1172 (1992).
[27] L. Burlachkov *et al.*, Phys. Rev. B **50**, R16770 (1994).
[28] M. V. Feigel'man and V. M. Vinokur, Phys. Rev. B **41**, 8986 (1990).
[29] E. A. Pashitskii *et al.*, Fiz. Nizk. Temp. **27**, 131 (2001) [Low Temp. Phys. **27**, 96 (2001)].